

Volkov-Pankratov states in a driven semimetal for a generic interface

Aiman Rauf¹ and SK Firoz Islam¹

¹*Department of Physics, Jamia Millia Islamia, New Delhi-110025, INDIA*

Volkov-Pankratov states are the non-topological massive bound states which generally arise across the smooth interface between two adjacent regions of a two-band semimetal, over which a gap parameter changes sign smoothly. In this work, we show that these modes can be engineered even for a generic smooth interface without any sign inversion. We consider a threefold and a twofold topological semimetal in which two adjacent regions are illuminated by light from two different sources with different light parameters (amplitudes, frequency, phase etc). We show that the interface can exhibit a quantum well for a certain parameter regime even without any sign change of the gap term. Such quantum well can host a number of Volkov-Pankratov states. Finally, we discuss the stability of these states against the deformation of the interfacial well and its transport signatures (Ramsauer Townsend effect).

I. INTRODUCTION

The gapless one-dimensional (1D) edge modes or two-dimensional (2D) surface states with insulating bulk are the hallmarks of the 2D and 3D topological insulator, respectively. Prior to the discovery of such materials, in the early 1980s, Volkov and Pankratov showed that an interface between two regions of a gapless two-band semimetal with mutually inverted mass term gives rise to a number of localized massive bound states[1, 2] in addition to the topological states. These massive states are non-topological in nature and dubbed as Volkov Pankratov (VP) states [3]. Note that abrupt sign change generally gives rise to a pair of topologically protected chiral modes instead of massive VP states. A number of theoretical works were carried out in recent time, predicting massless 1D chiral topological modes in 2D Dirac-type materials with the inverted mass term [4–6], where the mass term changes sign abruptly. Unidirectional chiral interfacial electromagnetic wave has been also predicted in a broken time reversal symmetric Weyl semimetal [7]. For the smooth interface, the VP states were obtained in photonic graphene with an inverted mass term [8]. In recent times, a series of theoretical works investigating the VP states in different types of newly emerged electronic systems have been carried out [3, 9–12]. Very recently, several experimental observations of the VP states were also reported[13, 14].

The last decade has witnessed a sharp increase in the research interest in periodically driven fermionic systems, especially after the discovery of Floquet topological insulator. The application of light or irradiation to an electronic system can break time reversal symmetry and lead to a non-trivial topological phase-Floquet topological insulator. Following the proposal of photoinduced topological phase transition [15], followed by its experimental discovery [16–19], a series of theoretical investigations were carried out in this direction [20–27]. The Floquet theory [28] provides a mathematical framework to study system's evolution over time and the modulated band structure in the presence of time periodic external perturbation. Periodically driven non-equilibrium electronic

system has diverse application, namely- shining light on the normal region of a Josephson junction can induce a $0 - \pi$ phase transition in its transport signatures[29, 30], manipulating spin and valley degrees of freedom in different types of electronic systems [31–36]. A series of theoretical works also revealed the possibility of photo tunability of Weyl nodes [37–41].

The Weyl semimetal is a new class of 3D topological material that has gained intense research interest in the last decade, because of its unique band structure and transport signatures[42, 43]. Its electronic properties are described by the Weyl equation, instead of Schrödinger's equation. Apart from usual two-band Weyl semimetal, another intriguing class of 3D topological material is the recently discovered three-fold topological semimetals[44]. Contrary to two-band Weyl semimetal, these semimetals exhibit a dispersionless flat band in addition to the conic bands. Photo driven band structure modulation and interfacial chiral modes were studied in recent times in this material [45]. In this work, we consider two and three-band topological semimetals and consider an interface between the two adjacent regions which are driven by the irradiation from two different sources with different light parameters. We note that an interfacial quantum well can emerge for certain parameter regime even without any sign change of light induced symmetry breaking parameter. The interface is considered to be smooth which gives rise to the VP states. We obtain exact analytical solutions for the VP states across the smooth boundary in both materials. We also discuss that although such VP states are non topological in nature, any weak deformation of the interfacial quantum well does not affect the VP modes. Finally we also discuss that such modes can be detected by analyzing the unit transmission of an incoming electron over such interfacial well.

The remainder of this paper is organized as follows. In Sec.(II), we discuss the low energy effective Hamiltonian of the threefold semimetal and its energy spectrum. The Sec. (II A) briefly introduces the Floquet theory and then we revisit the band structure modulation of irradiated three-fold semimetal. We investigate the interfacial modes for smooth interface in the Sec. (II B). Finally we

summarize in the Sec. (V)

II. THREE DIMENSIONAL THREE-FOLD SEMIMETALS

First we consider a gapless three-fold 3D semimetals (TSM) [44] that can be regarded as 3D counterpart of the 2D dice lattice[46–48]. One of the notable features of TSM is the presence of dispersionless flat band in addition to linearly dispersive conic bands. The low energy effective Hamiltonian for such material was obtained by using symmetry analysis as [44, 49]

$$H = v \begin{bmatrix} 0 & e^{i\phi}k_z & e^{-i\phi}k_y \\ e^{-i\phi}k_z & 0 & e^{i\phi}k_x \\ e^{i\phi}k_y & e^{-i\phi}k_x & 0 \end{bmatrix} \quad (1)$$

where v is the Fermi velocity, ϕ is the real parameter and $c = \hbar = k_B = 1$ has been used throughout the calculations. Inside the first Brillouin zone, there exists four such nodal points among which we consider only one. The band is non-degenerate at $k \neq 0$, unless $\phi = n\pi/3$ where n is an integer. Again for $\pi/3 < \phi < 2\pi/3$, the Hamiltonian can be adiabatically connected to the one for $\phi = \pi/2$ for which the Hamiltonian can be re-written as $H = v\mathbf{k}\cdot\mathbf{S}$. Here, $\mathbf{k} \equiv \{k_x, k_y, k_z\}$ is the 3D momentum operator and $\mathbf{S} \equiv \{S_x, S_y, S_z\}$ is the pseudospin-1 matrix given by

$$S = i \begin{bmatrix} 0 & e_z & -e_y \\ -e_z & 0 & e_x \\ e_y & -e_x & 0 \end{bmatrix} \quad (2)$$

The energy spectrum disperses linearly with a dispersionless flat band, given by $E_{\lambda,\mathbf{k}} = \lambda v|\mathbf{k}|, 0$ where $\lambda = \pm$ denote conduction and valence bands, and flat band corresponds to the zero level.

A. Floquet Hamiltonian and energy spectrum of threefold semimetal

In this section, we briefly review the band structure modulation of irradiated TSM, based on Floquet theory [28], within high-frequency limit. Consider a TSM being exposed to an external time-dependent perturbation in the form of irradiation or light propagating along the z -direction. The irradiation, described by a vector potential $A(t) = [A_x \sin(\Omega t), A_y \sin(\Omega t - \delta), 0]$, where Ω is the frequency of the irradiation and δ is the phase, induces effects on the non-perturbed Hamiltonian by adjusting the canonical momentum as $\mathbf{k} \rightarrow \mathbf{k} + e\mathbf{A}(t)$ where e represents the electron charge. To solve this irradiated Hamiltonian, we employ the Floquet theory which states that perturbed Hamiltonian exhibits a set of orthonormal solutions $\psi(t) = \phi(t)e^{-i\epsilon t}$, where $\phi(t) = \phi(t + T)$, T is the field period, and ϵ denotes Floquet quasi-energy. Expanding the Floquet states $\phi(t)$ as a

sum over Fourier components or Floquet side-band indices ($\phi(t) = \sum_n \phi_n(t)e^{in\Omega t}$), allows for the determination of the quasi-energy spectrum by diagonalizing the Floquet Hamiltonian based on the Floquet side bands ‘ n ’. In the high-frequency limit, an effective Hamiltonian, H_{eff} , is derived using the Floquet-Magnus expansion [28], represented as $H_{eff} \simeq H + H_F^{(1)} + \dots$, where $H_F^{(1)} = [H^-, H^+]/\Omega$ is the first order correction with

$$H_m = \frac{1}{T} \int_0^T V(t)e^{-im\Omega t} dt \quad (3)$$

and $m = \pm 1$. After simplifying, the effective Hamiltonian can be written as $H_{eff} = H + vS_z\gamma$ where $\gamma = ve^2(2\Omega)^{-1}A_x A_y \sin\delta$. The energy spectrum of the effective Floquet Hamiltonian comes out to be $\epsilon_{\lambda,k} = \lambda v\sqrt{k_x^2 + k_y^2 + (k_z + \gamma)^2}$. The external perturbation does not lead to any gap formation, as noted in the case of irradiated graphene, rather causes a momentum shift along the direction of light propagation. The momentum shift can be controlled by tuning the phase of light, amplitude as well as the frequencies.

B. Interfacial modes

1. Interfacial VP states for threefold topological semimetals

To study VP states, we drive the two adjacent regions of TSM by fast oscillating laser field from two different sources, which means that the momentum shifts are not same in the both regions. We would like to recall that the interfacial modes for an abrupt interface in 3D threefold semimetal have been studied in Ref. [45] by one of us, where the photoinduced momentum shift changes sign across the boundary. Contrary to this, here we consider that the light induced momentum shift in two regions are γ_1 and γ_2 , respectively i.e., the boundary is very generic and the momentum shift may not changes sign. These two regions are separated by a smooth interface of width L over which the momentum shift γ_1 changes to γ_2 . Let's consider that the interface is in the $y - z$ plane at $x = 0$. In such case, the momentum shift can be modelled as $\gamma(x) = \gamma_a + \gamma_r \tanh(x/L)$ where L is the width of the interface, $\gamma_a = (\gamma_1 + \gamma_2)/2$ is the average of the momentum shift in two regions and $\gamma_r = (\gamma_1 - \gamma_2)/2$ is the relative difference between the same. From hereafter, we shall set $v = 1$. For such smooth interface, after decoupling the eigen value equation, we arrive at

$$\left[-\frac{\partial^2}{\partial x^2} + V_{3f}(x) \right] \psi_2 = [E^2 - k_y^2 - k_z^2 - \gamma_r^2] \psi_2 \quad (4)$$

where the potential $V_{3f}(x) = -U(E) \text{sech}^2(x/L) + 2\gamma_r(k_z + \gamma_a) \tanh(x/L)$ with $U(E) = \gamma_r k_y / EL + \gamma_r^2$. This potential is well-known Rosen-Morse potential [50]. There exists a region of momentum satisfying $U(E) > 0$

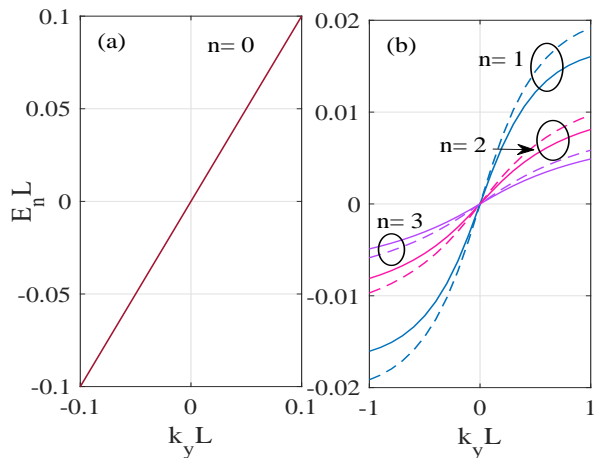


FIG. 1. The interfacial bound states for (a) $n = 0$. This is the gapless unidirectional chiral mode that is topological in nature and does not depend the nature of boundary details. (b) The dispersion of non-topological VP modes corresponding to $n = 1, 2, 3$. Here, two sets of boundary parameters are used as $(\gamma_a, \gamma_r) = (0.3, 0.1)$ -solid line and $(0.32, 0.12)$ -dashed-line. These VP modes are significantly affected by the slight changes of the boundary details, confirming the non-topological nature. In both cases we set $k_z = 0$.

and $|\gamma_r(k_z + \gamma_a)| < U$ for which the potential acts as a well instead of a barrier. The bound states formed inside the well satisfy the following equation

$$E_n^2 = k_y^2 + (k_z + \gamma_a)^2 + \gamma_r^2 - \frac{\Gamma^2(E, n)}{4L^2} - \frac{4(k_z + \gamma_a)^2 L^2 \gamma_r^2}{\Gamma^2(E, n)} \quad (5)$$

where $\Gamma(E, n) = \sqrt{4U(E)L^2 + 1} - (2n + 1)$. The above equation is a transcendental equation of energy, which has to be solved numerically to find the bound states solutions. The above expression of bound states can be seen to be strongly anisotropic in $k_y - k_z$ space. In order to analyze these modes, we numerically plot first few modes ($n = 0, 1, 2, 3$) versus k_y and k_z , separately in Fig. (1). First we plot the zeroth ($n = 0$) mode using Eq. (5) in Fig. (1a). This is topological mode which is insensitive to the boundary details i.e., does not depend on the parameters (γ_a, γ_r) . We note that the zeroth mode disperses linearly and is unidirectional in nature. Note that the topological mode was also obtained for abrupt interface as well as for smooth interface but with inverted momentum shift in Ref. (45). On the contrary in the present case the boundary is very generic i.e., momentum shift does not change sign. For example, for the Fig. (1), we have taken the boundary parameters as $(\gamma_a L, \gamma_r L) = (0.3, 0.1)$ which corresponds to $\gamma_1 L = 0.4$ and $\gamma_2 L = 0.2$. Here, the momentum shift γ does not change sign rather just smoothly jumps from $\gamma_1 L = 0.4$ to $\gamma_2 L = 0.2$. The VP states are also plotted in Fig. (1b) correspond to $n = 1, 2, 3$. These modes are very sensitive to the boundary parameters as shown by the solid

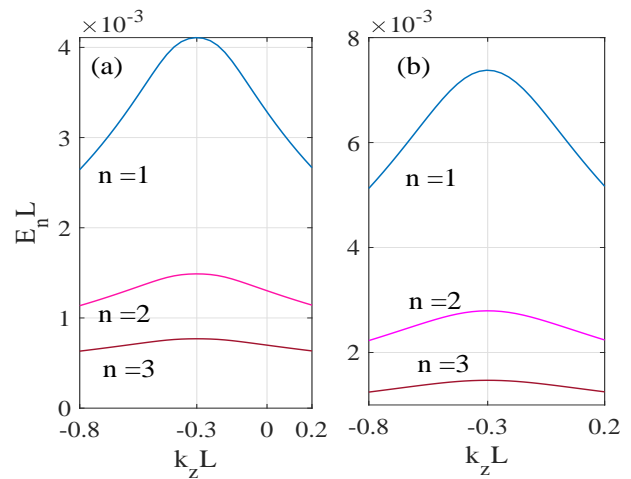


FIG. 2. The first few VP states are plotted with k_z for (a) $k_y L = 0.1$ and (b) $k_y L = 0.2$, respectively. Here we kept non-zero k_y in order to widen the range of k_z as given by $|k_z| < k_y/E + \gamma_r - \gamma_a$. We also keep the same boundary parameters as $(\gamma_a, \gamma_r) = (0.3, 0.1)$. The VP states are very weakly varying with k_z and exhibit a maxima at $k_z = -\gamma_a$.

and dashed lines correspond to two sets of boundary parameters $(\gamma_a L, \gamma_r L) = (0.3, 0.1)$ and $(0.32, 0.12)$. It is noteworthy to mention that these VP states are also unidirectional and chiral, which is unique contrary to the system like graphene [8]. Note that the number of 'n's are limited by the condition $E_n^2 > 0$ so that the energy is always real.

The behaviour of the VP states with k_z are also shown in Fig. (2) for two sets of k_y as $k_y L = 0.1$ and $k_y L = 0.2$. Here k_y is taken to be non-zero just to keep a wide range of k_z corresponding to interfacial potential well instead of barrier, as defined by $|k_z| < k_y/EL + \gamma_r - \gamma_a$. We note that VP states are very weakly varying with k_z and the solution is restricted to positive energy only because of the aforementioned condition. We also note that no zero mode solution appears here. It can be understood from the fact that the zero mode is a topological mode and it does not depend on the type of interface. For abrupt interface with inverted momentum shift, an exact solution for zero mode was found in Ref. (45) as $E_0 = \text{sgn}(\gamma)k_y$ which has no dispersion with k_z that is exactly what we obtain for the smooth generic interface in Fig. (1a). With changing k_y , the behaviour remains almost unaffected except a mismatch in the amplitude. However, the lowest VP modes are relatively most sensitive with k_z

2. Interfacial modes in two-fold semimetal

In this section, we discuss the the VP states for a two-band 3D topological semimetal, namely the Weyl semimetal. This material has been in the focus of research community in recent times [42]. The low energy effective Hamiltonian of a two-fold 3D WSM around a

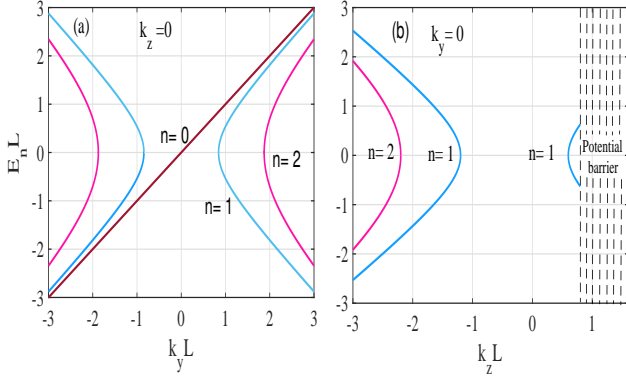


FIG. 3. The VP states for (a) $k_z = 0$ and (b) $k_y = 0$ for $(\gamma_a L, \gamma_r L) = (0.3, 0.1)$.

particular Weyl node can be taken as $H = \sigma \cdot \mathbf{k}$ with linearly dispersive energy eigen values $E_{\lambda, k} = \lambda|k|$, where $\sigma = (\sigma_x, \sigma_y, \sigma_z)$ are Pauli matrices in orbital space. The effects of a fast oscillatory laser field can be treated by Floquet theorem within high-frequency limit which yields Floquet energy spectrum $\varepsilon_{\lambda, k} = \lambda\sqrt{k_x^2 + k_y^2 + (k_z + \gamma)^2}$. Note that unlike the case of threefold semimetal, here the flat band does not exist. After squaring the eigen value equation we arrive at

$$\left[-\frac{\partial^2}{\partial x^2} + V_w(x) \right] \psi = (E^2 - \gamma_r^2 - k_y^2 - k_z^2) \psi \quad (6)$$

where

$$V_w(x) = -\gamma_r \left(\gamma_r + \frac{1}{L} \right) \text{sech}^2\left(\frac{x}{L}\right) + 2\gamma_r(k_z + \gamma_a) \tanh\left(\frac{x}{L}\right). \quad (7)$$

This potential mimics the well-known Rosen-Morse potential well for $|\gamma_r(k_z + \gamma_a)| < \gamma_r(\gamma_r + 1/L)$ which for $\gamma_r > 0$ gives a restriction on k_z as $|k_z| < (1/L + \gamma_r - \gamma_a)$. Note that the region $|k_z| > (1/L + \gamma_r - \gamma_a)$ corresponds to potential barrier instead of well. The bound state energy inside this well can be immediately obtained as

$$E_n^2 = k_y^2 + (k_z + \gamma_a)^2 + \gamma_r^2 - \left(\gamma_r - \frac{n}{L} \right)^2 - \frac{\gamma_r^2(k_z + \gamma_a)^2}{\left(\gamma_r - \frac{n}{L} \right)^2}. \quad (8)$$

The zeroth mode ($n = 0$) can be easily found to be $E_0 = \text{sgn}(\gamma_r)k_y$ which is gapless, topological and does not depend on the boundary details. Whereas, $n = 1, 2, 3..$ modes are sensitive to the boundary width L and non-topological in nature, these modes are purely due to the smooth nature of the boundary-known as the VP modes. Note that only those ‘ n ’s are allowed for which $E_n^2 > 0$ i.e., E_n is real. Apart from the zeroth ($n = 0$) topological chiral mode, first few VP modes are also shown in the Fig. (3a) for $k_z = 0$ which are almost hyperbolic in nature and symmetric about $k_y = 0$. On the other hand, for $k_y = 0$ only $n = 1$ mode appears for $k_z > 0$

[see Fig. (3b)]. However, the $n > 1$ modes do not appear in this region as it does not satisfy the condition $E_n^2 > 0$ and $|k_z| < (1/L + \gamma_r - \gamma_a)$ simultaneously, but these higher VP modes are present in the $k_z < 0$ region respecting both the aforementioned conditions. Overall, one can see a strong asymmetry in VP modes with respect to $k_z = 0$ point.

We can quickly draw a comparison between VP states appear in the threefold and two-fold Weyl semimetal. Contrary to the case of TSM, here the depth of the interfacial potential well, $\gamma_r(\gamma_r + 1/L)$, does not depend on the transverse momentum (k_y). Additionally, the the VP states for Weyl semimetal are not unidirectional chiral whereas for TSM they are.

3. VP states for generic interface in graphene

Finally, we comment on the generic boundary VP states for the case in a 2D two-band semimetals like graphene. Unlike the case of 3D semimetals, application of light propagating along the direction normal to the plane of a 2D sheet of monolayer graphene opens up a topological gap in graphene [15]. If two neighbouring regions of graphene are exposed to the fast oscillating laser field from two different sources, two dissimilar mass terms emerge in those regions, respectively. Consider that these two mass terms are γ_1 and γ_2 which smoothly change from one to another across a boundary of width L . We can immediately model the mass term in the same fashion as the momentum shift in the previous cases, as $\gamma(x) = \gamma_a + \gamma_r \tanh(x/L)$. In this case, the interfacial potential-well can be obtained as

$$V_g(x) = -\gamma_r \left(\gamma_r + \frac{1}{L} \right) \text{sech}^2\left(\frac{x}{L}\right) - 2\gamma_r\gamma_a \tanh\left(\frac{x}{L}\right) \quad (9)$$

which is just the $k_z = 0$ case for Weyl semimetal as expected, see Eq. (7). This potential well exhibits a minima when $|\gamma_r\gamma_a| < \gamma_r(\gamma_r + 1/L)$ and the bound states inside it can be obtained by just setting $k_z = 0$ in Eq. (8) as

$$E_n^2 = k_y^2 + \gamma_a^2 + \gamma_r^2 - \left(\gamma_r - \frac{n}{L} \right)^2 - \frac{\gamma_r^2\gamma_a^2}{\left(\gamma_r - \frac{n}{L} \right)^2}. \quad (10)$$

These are the bound state energies which arise inside the interfacial Rosen-Morse potential well for a generic boundary even without any sign change in the mass term. We can quickly check that the zeroth topological mode $E_0 = \text{sgn}(\gamma_r)k_y$ whereas the $n > 1$ modes are non-topological and sensitive to the boundary details-known as the VP modes. If we consider the interface across which the topological mass term changes sign, we can set $\gamma_a = 0$ and $\gamma_r = \gamma$ in Eq. (10) that will return the well-known VP states [8]

$$E_n = \pm \sqrt{k_y^2 + 2\gamma \frac{|n|}{L} - \frac{n^2}{L^2}} \quad (11)$$

provided $(k_y L)^2 + 2\gamma L|n| > n^2$. Here, the VP states correspond to different n exhibit different gap in its band spectrum.

III. STABILITY OF THE VP STATES

The VP states are non-topological in nature as they depend on the details of the interface of width L . Hence one could expect that VP states might be suppressed by a small deformation of the interfacial Rosen-Morse or Pöschl-Teller potential well. We can quickly check the case of deformed potential well which is in fact the more realistic situation. In order to do so, the smooth change of the momentum shift or mass term can be modelled by using a deformed tangent hyperbolic function as $\gamma_r(x) = \gamma_a + \gamma_r \tanh_r(x)$. The deformed hyperbolic functions are defined as: $\sinh_r(x) = (e^x - r e^{-x})/2$ and $\cosh_r(x) = (e^x + r e^{-x})/2$ where $1 > r > 0$ describes the degree of deformation. Such deformed hyperbolic functions, introduced by Arai [51], satisfy the relation $1 - \tanh_r^2(x) = r \operatorname{sech}_r^2(x)$, $\cosh_r^2(x) - \sinh_r^2(x) = r$ and $\frac{d}{dx} \tanh_r(x) = r \operatorname{sech}_r^2(x)$. The bound state solutions for deformed Rosen-Morse or Pöschl-Teller potential well can be shown to be insensitive to the degree of deformation r [52]. Hence, we can conclude that although the VP states are non-topological but these are robust to the weak deformation of the interfacial potential well.

IV. TRANSPORT SIGNATURE AND EXPERIMENTAL FEASIBILITY

In this section, we briefly discuss the electron transmission through the interface. First we consider the case of transmission probability of an incoming electron with positive energy over the interfacial potential well which corresponds to the inverted mass term, for example let's consider the case of graphene. In such case, the interfacial well becomes Pöschl-Teller potential well instead of Rosen-Morse. The transmission probability for an incoming electron with energy (> 0) over the Pöschl-Teller potential well can be obtained as [53]

$$T(k_x, \gamma_r) = \frac{\sinh^2(\pi k_x L)}{\sinh^2(\pi k_x L) + \cos^2[\frac{\pi}{2}(2\gamma_r L + 1)]}. \quad (12)$$

It is interesting to note that an incident electron can fully pass over the well with $T = 1$ without any reflection when $\gamma_r = j$ with $j = 1, 2, 3, \dots$. This is well-known *Ramsauer-Townsend (RT)* effect. As the depth of the well is determined by $\gamma_r(\gamma_r + 1)$ which is in-fact purely determined by the light parameters, we can conclude that the unit transmission (*RT*-effect) can be achieved by just simply tuning light parameters externally. Note that $j = 0$ corresponds to the absence of the quantum well, hence it is

avoided. We note that those γ_r values ($\gamma_r = j$), for which the unit transmission occurs, correspond to the VP index n . We revisit here the *RT* effect over a 1D rectangular potential well of depth $-V_0$ and width L , where the unit transmission of electron occurs for the energy (E_n) of the incident electron satisfies $E_n + V_0 = n^2 \pi^2 / 2\pi L^2$. In contrast, the bound states here are dispersive along the free direction, and only a sets of γ_r 's allow unit transmission.

Now we consider the case of generic interface for which interfacial potential well is not Pöschl-Teller rather Rosen-Morse well. In such case the transmission of an incoming electron over the well can also obtained as [54]

$$T(k_x, \gamma_a, \gamma_r) = \frac{\sinh(\pi k_x L) \sinh(\pi q_x L)}{\sin^2(\pi \gamma_r L) + \sinh^2[\frac{\pi L}{2}(k_x + q_x)]} \quad (13)$$

where $q_x = \sqrt{k_x^2 - 2\gamma_r \gamma_a}$, which for inverted mass term i.e., $\gamma_a = 0$ reduces to the Eq. (12). Note that for inverted mass term the transmission probability $T = 1$ for $\gamma_r L = 1, 2, 3, \dots$ whereas for generic interface it is exhibiting maxima periodically for the same values of $\gamma_r L$. The number of such maxima could be regarded as the consequence of the existence of the VP states inside the well, and well-known *RT*-effect.

Finally we comment on the experimental feasibility of realizing VP states. The typical photon energy that is generally needed to perturb a quantum system is about 0.25 eV with $eA_0 = 0.01 - 0.2 \text{ \AA}^{-1}$. The light parameters belonging to this regime can be used for studying VP states. The recent reported experiment [13, 14] on identifying the VP states is particularly designed for VP states resulted from the inverted mass term. In addition to these experiments, the *RT*-effect can also be used to identify the VP states.

V. CONCLUSION

We studied the VP states in two and three fold topological semimetals for a very generic interface instead of changing the sign of mass term or momentum shift. In order to induce the momentum shift in 3D semimetals or mass term in 2D semimetals (graphene), we drive the two neighbouring regions of the system by periodically time-dependent perturbation in the form of fast oscillating laser field by using two different sources which results in two dissimilar mass terms or momentum shifts. We note that there exists a certain momentum or parameters range for which the interface can act as a quantum well and host a number of massive bound states known as VP states. Finally, we also discuss that the interfacial well for inverted mass term can give a unit transmission for incoming electron with energy above the well-known as *RT* effect. This effect might be used to probe these VP states. These results are in complete contrast with the existing literature of understanding such VP states.

-
- [1] V. A. Volkov and O. A. Pankratov, “Two-dimensional massless electrons in an inverted contact,” *JETP Lett.* **42**, 178 (1985).
- [2] O.A. Pankratov, S.V. Pakhomov, and B.A. Volkov, “Supersymmetry in heterojunctions: Band-inverting contact on the basis of pb1xsnxte and hg1xcdxte ,” *Solid State Communications* **61**, 93–96 (1987).
- [3] S. Tchoumakov, V. Jouffrey, A. Inhofer, E. Bocquillon, B. Plaçais, D. Carpentier, and M. O. Goerbig, “Volkov-pankratov states in topological heterojunctions,” *Phys. Rev. B* **96**, 201302 (2017).
- [4] Y. Kim, K. Choi, J. Ihm, and H. Jin, “Topological domain walls and quantum valley hall effects in silicene,” *Phys. Rev. B* **89**, 085429 (2014).
- [5] G. W. Semenoff, V. Semenoff, and Fei Zhou, “Domain walls in gapped graphene,” *Phys. Rev. Lett.* **101**, 087204 (2008).
- [6] H. L. Calvo, L. E. F. Foa Torres, P. M. Perez-Piskunow, C. A. Balseiro, and Gonzalo Usaj, “Floquet interface states in illuminated three-dimensional topological insulators,” *Phys. Rev. B* **91**, 241404 (2015).
- [7] A. A. Zyuzin and V. A. Zyuzin, “Chiral electromagnetic waves in weyl semimetals,” *Phys. Rev. B* **92**, 115310 (2015).
- [8] F. D. M. Haldane and S. Raghu, “Possible realization of directional optical waveguides in photonic crystals with broken time-reversal symmetry,” *Phys. Rev. Lett.* **100**, 013904 (2008).
- [9] D. J. Alspaugh, D. E. Sheehy, M. O. Goerbig, and P. Simon, “Volkov-pankratov states in topological superconductors,” *Phys. Rev. Res.* **2**, 023146 (2020).
- [10] D. K. Mukherjee, D. Carpentier, and M. O. Goerbig, “Dynamical conductivity of the fermi arc and the volkov-pankratov states on the surface of weyl semimetals,” *Phys. Rev. B* **100**, 195412 (2019).
- [11] X. Lu and M. O. Goerbig, “Dirac quantum well engineering on the surface of a topological insulator,” *Phys. Rev. B* **102**, 155311 (2020).
- [12] T. L. van den Berg, A. De Martino, M. R. Calvo, and D. Bercioux, “Volkov-pankratov states in topological graphene nanoribbons,” *Phys. Rev. Res.* **2**, 023373 (2020).
- [13] A. Inhofer, S. Tchoumakov, B. A. Assaf, G. Fève, J. M. Berroir, V. Jouffrey, D. Carpentier, M. O. Goerbig, B. Plaçais, K. Bendias, D. M. Mahler, E. Bocquillon, R. Schlereth, C. Brüne, H. Buhmann, and L. W. Molenkamp, “Observation of volkov-pankratov states in topological HgTe heterojunctions using high-frequency compressibility,” *Phys. Rev. B* **96**, 195104 (2017).
- [14] J. Bermejo-Ortiz, G. Krizman, R. Jakiela, Z. Khosravizadeh, M. Hajlaoui, G. Bauer, G. Springholz, L.-A. de Vaultier, and Y. Guldner, “Observation of weyl and dirac fermions at smooth topological volkov-pankratov heterojunctions,” *Phys. Rev. B* **107**, 075129 (2023).
- [15] T. Oka and H. Aoki, “Photovoltaic hall effect in graphene,” *Phys. Rev. B* **79**, 081406 (2009).
- [16] N H Lindner, G. Refael, and V. Galitski, “Floquet topological insulator in semiconductor quantum wells,” *Nature Phys.* **7**, 490 (2011).
- [17] Y.-G. Peng, C.-Z. Qin, D.-G. Zhao, Y.-X. Shen, X.-Y. Xu, M. Bao, H. Jia, and X.-F. Zhu, “Experimental demonstration of anomalous Floquet topological insulator for sound,” *Nature Com.* **7**, 13368 (2016).
- [18] H. Zhang, J. Yao, J. Shao, H. Li, S. Li, D. Bao, C. Wang, and G. Yang, “Anomalous photoelectric effect of a polycrystalline topological insulator film,” *Sci. rep.* **4**, 5876 (2014).
- [19] Y. Wang, H. Steinberg, P. Jarillo-Herrero, and N. Gedik, “Observation of Floquet-Bloch states on the surface of a topological insulator,” *Science* **342**, 453–457 (2013).
- [20] J. Inoue and A. Tanaka, “Photoinduced spin Chern number change in a two-dimensional quantum spin Hall insulator with broken spin rotational symmetry,” *Phys. Rev. B* **85**, 125425 (2012).
- [21] X. Zhai and G. Jin, “Photoinduced topological phase transition in epitaxial graphene,” *Phys. Rev. B* **89**, 235416 (2014).
- [22] M. Ezawa, “Photoinduced Topological Phase Transition and a Single Dirac-Cone State in Silicene,” *Phys. Rev. Lett.* **110**, 026603 (2013).
- [23] P. M. Perez-Piskunow, G. Usaj, C. A. Balseiro, and L. E. F. F. Torres, “Floquet chiral edge states in graphene,” *Phys. Rev. B* **89**, 121401 (2014).
- [24] B. Dey and T. K. Ghosh, “Floquet topological phase transition in the $\alpha-T_3$ lattice,” *Phys. Rev. B* **99**, 205429 (2019).
- [25] SK. F. Islam and A. Saha, “Driven conductance of an irradiated semi-dirac material,” *Phys. Rev. B* **98**, 235424 (2018).
- [26] Runnan Zhang, Ken-ichi Hino, Nobuya Maeshima, Haruki Yogemura, and Takeru Karikomi, “Laser-induced surface magnetization in floquet-weyl semimetals,” *Phys. Rev. B* **108**, 155308 (2023).
- [27] T. Deng, B. Zheng, F. Zhan, J. Fan, X. Wu, and R. Wang, “Photoinduced floquet mixed-weyl semimetallic phase in a carbon allotrope,” *Phys. Rev. B* **102**, 201105 (2020).
- [28] André Eckardt, “Colloquium: Atomic quantum gases in periodically driven optical lattices,” *Rev. Mod. Phys.* **89**, 011004 (2017).
- [29] X. Zhou and G. Jin, “Light-modulated $0-\pi$ transition in a silicene-based Josephson junction,” *Phys. Rev. B* **94**, 165436 (2016).
- [30] U. Khanna, S. Rao, and A. Kundu, “ $0-\pi$ transitions in a Josephson junction of an irradiated Weyl semimetal,” *Phys. Rev. B* **95**, 201115 (2017).
- [31] A. López, Z. Z. Sun, and J. Schliemann, “Floquet spin states in graphene under ac-driven spin-orbit interaction,” *Phys. Rev. B* **85**, 205428 (2012).
- [32] M. Dey, S. Sarkar, and S. K. Maiti, “Light irradiation controlled spin selectivity in a magnetic helix,” *Phys. Rev. B* **108**, 155408 (2023).
- [33] A. Kundu, H. A. Fertig, and B. Seradjeh, “Floquet-Engineered Valleytronics in Dirac Systems,” *Phys. Rev. Lett.* **116**, 016802 (2016).
- [34] L. E. Golub, S. A. Tarasenko, M. V. Entin, and L. I. Margarill, “Valley separation in graphene by polarized light,” *Phys. Rev. B* **84**, 195408 (2011).
- [35] B. Dey and T. K. Ghosh, “Photoinduced valley and electron-hole symmetry breaking in $\alpha-T_3$ lattice: The role of a variable Berry phase,” *Phys. Rev. B* **98**, 075422 (2018).

- [36] M. Tahir, A. Manchon, and U. Schwingenschlögl, “Photoinduced quantum spin and valley Hall effects, and orbital magnetization in monolayer MoS₂,” *Phys. Rev. B* **90**, 125438 (2014).
- [37] Z. Yan and Z. Wang, “Tunable Weyl Points in Periodically Driven Nodal Line Semimetals,” *Phys. Rev. Lett.* **117**, 087402 (2016).
- [38] X.-X. Zhang, T.-T. Ong, and N. Nagaosa, “Theory of photoinduced floquet weyl semimetal phases,” *Phys. Rev. B* **94**, 235137 (2016).
- [39] B. Chen, R. Zhou and D.-H. Xu, “Floquet Weyl semimetals in light-irradiated type-II and hybrid line-node semimetals,” *Phys. Rev. B* **97**, 155152 (2018).
- [40] A. Narayan, “Tunable point nodes from line-node semimetals via application of light,” *Phys. Rev. B* **94**, 041409 (2016).
- [41] M. Ezawa, “Photoinduced topological phase transition from a crossing-line nodal semimetal to a multiple-Weyl semimetal,” *Phys. Rev. B* **96**, 041205 (2017).
- [42] N. P. Armitage, E. J. Mele, and Ashvin Vishwanath, “Weyl and dirac semimetals in three-dimensional solids,” *Rev. Mod. Phys.* **90**, 015001 (2018).
- [43] A.A. Burkov, “Weyl metals,” *Annual Review of Condensed Matter Physics* **9**, 359–378 (2018).
- [44] Barry Bradlyn, Jennifer Cano, Zhijun Wang, M. G. Vergniory, C. Felser, R. J. Cava, and B. Andrei Bernevig, “Beyond dirac and weyl fermions: Unconventional quasiparticles in conventional crystals,” *Science* **353** (2016), 10.1126/science.aaf5037.
- [45] SK. F. Islam and A. A. Zyuzin, “Photoinduced interfacial chiral modes in threefold topological semimetal,” *Phys. Rev. B* **100**, 165302 (2019).
- [46] A. Raoux, M. Morigi, J.-N. Fuchs, F. Piéchon, and G. Montambaux, “From dia- to paramagnetic orbital susceptibility of massless fermions,” *Phys. Rev. Lett.* **112**, 026402 (2014).
- [47] Balázs Dóra, Janik Kailasvuori, and R. Moessner, “Lattice generalization of the dirac equation to general spin and the role of the flat band,” *Phys. Rev. B* **84**, 195422 (2011).
- [48] SK Firoz Islam and Paramita Dutta, “Valley-polarized magnetoconductivity and particle-hole symmetry breaking in a periodically modulated $\alpha - \sqcup_3$ lattice,” *Phys. Rev. B* **96**, 045418 (2017).
- [49] Miguel-Ángel Sánchez-Martínez, Fernando de Juan, and Adolfo G. Grushin, “Linear optical conductivity of chiral multifold fermions,” *Physical Review B* **99** (2019), 10.1103/physrevb.99.155145.
- [50] N. Rosen and Philip M. Morse, “On the vibrations of polyatomic molecules,” *Phys. Rev.* **42**, 210–217 (1932).
- [51] A. Arai, “Exactly solvable supersymmetric quantum mechanics,” *J. Math. Anal. Appl.* **158**, 63 – 79 (1991).
- [52] H. Eğrifles, D. Demirhan, and F. Büyükkılıç, “Exact solutions of the schrödinger equation for the deformed hyperbolic potential well and the deformed four-parameter exponential type potential,” *Phys. Lett. A* **275**, 229 – 237 (2000).
- [53] L. D. Landau and E. M. Lifshitz, *Quantum mechanics: non-relativistic theory*, Vol. 3 (Elsevier, 2013).
- [54] F. L. Freitas, “Generalization of legendre functions applied to rosen-morse scattering states,” (2023), arXiv:2312.15652 [quant-ph]